Expression of Voltage-Gated Potassium Channels in Human and Mouse Colonic Carcinoma

Jiraporn Ousingsawat,[1] Melanie Spitzner,[1] Supaporn Puntheeranurak,[1] Luigi Terracciano,[2] Luigi Tornillo,[2] Lukas Bubendorf,[2] Karl Kunzelmann,[1] and Rainer Schreiber[1]

Abstract

Purpose: Voltage-gated Kv potassium channels, like ether a go-go (EAG) channels, have been recognized for their oncogenic potential in breast cancer and other malignant tumors.

Experimental Design: We examined the molecular and functional expression of Kv channels in human colonic cancers and colon of mice treated with the chemical carcinogens dimethylhydrazine and *N*-methyl-*N*-nitrosourea. The data were compared with results from control mice and animals with chemically induced DSS colitis.

Results: Electrogenic salt transport by amiloride-sensitive Na^+ channels and cyclic AMP–activated cystic fibrosis transmembrane conductance regulator Cl^- channels were attenuated during tumor development and colitis, whereas Ca^{2+}-dependent transport remained unchanged. Kv channels, in particular Eag-1, were enhanced during carcinogenesis. Multiplex reverse transcription-PCR showed increased mRNA expression for Kv1.3, Kv1.5, Kv3.1, and members of the Eag channel family, after dimethylhydrazine and *N*-methyl-*N*-nitrosourea treatment. Eag-1 protein was detected in the malignant mouse colon and human colonic cancers. Genomic amplification of Eag-1 was found in 3.4% of all human colorectal adenocarcinoma and was an independent marker of adverse prognosis.

Conclusions: The study predicts an oncogenic role of Kv and Eag channels for the development of colonic cancer. These channels may represent an important target for a novel pharmacotherapy of colonic cancer.

Membrane ion channels are essential for cell proliferation and have a role in the development of cancer. A substantial body of evidence exists that voltage-gated potassium (Kv) channels have an oncogenic function (1–4). Moreover, during carcinogenesis, changes in expression or activity of ion channels may affect electrolyte transport properties in epithelia, similar to the changes observed during inflammation (1). K^+ channels are involved in the development of cancer of prostate, colon, lung, and breast (1, 5). K^+ channels were identified in different cancer tissues, such as Ca^{2+}-activated and voltage-gated K^+ channels (Kv channel), the ether a go-go (Eag) family, and 2P-domain K^+ channels (1). However, Kv channels seem to play a central role in tumor cells, particularly in those of epithelial origin (1–3). Cell cycle–regulated Eag-1 channels, normally only expressed in excitable tissues and oocytes, are also found in cancer cells (4, 6, 7). Activation of these channels induces hyperpolarization of the plasma membrane, which may be essential for cell proliferation (2). Hyperpolarization of the membrane voltage facilitates Ca^{2+} signaling and is necessary for regulation of intracellular pH and cell volume. All of these variables (Ca^{2+}, pH, and volume) clearly affect cell proliferation (1, 2, 8).

Most studies on the oncogenic role of ion channels have been done in cell lines, leaving open their relevance for tumor development *in vivo*. We therefore designed the present study to examine the role of ion channels for tumor development *in vivo* in carcinogen-treated mice. Dimethylhydrazine (DMH) and *N*-methyl-*N*-nitrosourea (MNU) were used as carcinogenic agents. DMH is organotropic for the rodent colon. It is metabolized to methylazoxymethanol and methyldiazonium and causes methylation of nucleotides (9). Rectal application of MNU causes direct alkylation of DNA and also induces colonic tumors (10, 11). During the development of colon cancer, alterations in colonic electrolyte transport have been reported in previous studies (12, 13). Electrolyte transport seems to be affected in the premalignant colon, which may contribute to the irregularities in defecation, often observed in patients with human colonic cancer. We found that electrolyte transport was affected in colitis and during carcinogenesis. However, overexpression of cell cycle–regulated Eag-1 K^+ channels was only found in the premalignant mouse colon and in human colonic cancers.

Authors' Affiliations: [1]Institut für Physiologie, Universität Regensburg, Regensburg, Germany and [2]Institute for Pathology, University Hospital Basel, Basel, Switzerland

Received 8/4/06; revised 11/13/06; accepted 12/5/06.

Grant support: Deutsche Forschungsgemeinschaft SCHR 752/2-1 and Wilhelm Sander-Stiftung 2005.063.1.

The costs of publication of this article were defrayed in part by the payment of page charges. This article must therefore be hereby marked *advertisement* in accordance with 18 U.S.C. Section 1734 solely to indicate this fact.

Note: J. Ousingsawat and M. Spitzner contributed equally to the present study. K. Kunzelmann and R. Schreiber share senior authorship.

Requests for reprints: Karl Kunzelmann, Institut für Physiologie, Universität Regensburg, Universitätsstraβe 31, D-93053 Regensburg, Germany. Phone: 49-954-4302; Fax: 49-941-4315; E-mail: uqkkunze@mailbox.uq.edu.au.

doi:10.1158/1078-0432.CCR-06-1940

Materials and Methods

Patients, tumor material for fluorescence* in situ *hybridization analysis, and biological samples. Three hundred eighty-six surgically resected colorectal adenocarcinomas were selected from the files of the Institutes of Pathology of the University of Basel and from the Triemli Hospital, Zürich, Switzerland. Tissue microarray was constructed as previously described (14). Specimens were kept anonymous, and experiments were conducted according to the guidelines of the ethical committee of the University of Basel. Pathologic tumor-node-metastasis stage was determined according to the International Union Against Cancer (15). Colon biopsies were obtained from patients hospitalized at the Children's Hospital of the University of Freiburg/Germany and the Department of Internal Medicine of the University of Regensburg, according to the guidelines of the local ethical committee.

DMH, MNU, and DSS treatment. Animal studies were conducted according to the guidelines of the NIH guidelines for the care and use of animals in research and the German laws on protection of animals. C57BL/6NCrl mice were obtained from Charles River (Sulzfeld, Germany). DMH or control saline were dissolved in 0.9% saline and injected s.c. into the groin at a dose of 40 mg/kg once a week for 5 weeks. Proximal and distal colons were removed for RNA and protein isolation, histology, and functional measurements. For MNU treatment, mice were anesthetized by i.p. injection of ketamine/xylazine (120 mg/8 mg/kg × body weight). MNU (2.6 mg/0.4 mL of 0.9% NaCl solution) was given intrarectally twice a week for 2 weeks and once a week for additional 4 weeks. For potential difference measurements, a catheter (PE-10 tubing) containing ringer solution was inserted 2 cm into the rectum and perfused continuously at a rate of 1 mL/h. The catheter was attached via an agar bridge to an $AgCl^-$ electrode. A s.c. needle positioned in the abdomen and connected via an agar bridge served as the reference electrode. For DSS treatment of BALB/cOlaHsd mice, 3% DSS was added to drinking water for 7 to 10 days.

Histology. Mice were sacrificed under CO_2 inhalation; the colon was removed and stripped mechanically from submucosal tissues. Tissues were fixed for 20 min with 4% paraformaldehyde, 0.1% glutaraldehyde, 15% picric acid in PBS (pH 7.4) followed by a 12-h incubation in 4% paraformaldehyde, 15% picric acid in PBS (pH 7.4) at 4°C. Tissues were washed in PBS and incubated in 10%, 20%, and 30% sucrose solutions, dehydrated, and embedded in paraffin. Paraffin-embedded tissues were cut with a rotary microtome (Leica Mikrotom RM 2165, Wetzlar, Germany). Sections were dewaxed and rehydrated and stained with H&E. Some tissues were chock frozen in *iso*-pentane, sectioned at 5 μm, fixed with 4% paraformaldehyde in PBS (pH 7.4), and stained with hematoxylin.

Ussing chamber experiments. Stripped colon was put into ice cold bath solution [145 mmol/L NaCl, 0.4 mmol/L KH_2PO_4, 1.6 mmol/L K_2HPO_4, 6 mmol/L D-glucose, 1 mmol/L $MgCl_2$, 1.3 mmol/L Ca-gluconate (pH 7.4)] containing amiloride (20 μmol/L) and indomethacin (10 μmol/L). Tissues were mounted into an Ussing chamber with a circular aperture of 0.785 mm^2. Luminal and basolateral sides of the epithelium were perfused continuously at a rate of 5 mL/min. Bath solutions were heated to 37°C, using a water jacket. Experiments were carried out under open-circuit conditions. Data were collected continuously using PowerLab (ADInstruments, Spechbach, Germany). Values for transepithelial voltages (V_{te}) were referred to the serosal side of the epithelium. Transepithelial resistance (R_{te}) was determined by applying short (1s) current pulses (ΔI = 0.5 μA). R_{te} and equivalent short circuit currents (I_{SC}) were calculated according to Ohm's law ($R_{te} = \Delta V_{te}/\Delta I$, $I_{SC} = V_{te}/R_{te}$).

Crypt cell isolation and expression analysis of ion channels in colonic epithelial cells. Colonic crypts were isolated from an inverted colon in Ca^{2+}-free buffer solution. Total RNA was prepared from isolated crypts (NucleoSpin, Macherey-Nagel, Düren, Germany). After reverse transcription, semiquantitative multiplex reverse transcription-PCR was done. The following primers (accession no.) were used: mKv1.3 (NM_008418), 5′-GTACTTTGACCCACTCCGC -3′ (sense) and 5′-GCAAGCAAAGAACCGCACC-3′ (antisense); mKv1.5 (NM_145983), 5′-GCTACTTCGATCCCTTGAG -3′ (sense) and 5′-GCTCAAAAGTGAACCAGATC-3 (antisense); mKv3.1 (NM_008421), 5′-CCAGACGTACCGCTCGAC 3′ (sense) and 5′-CGAACAGCGCCCAGATGC-3′ (antisense); mEAG-1 (NM_010600), 5′-GGATTCTGCAAGCTGTCTG-3′ (sense) and 5′-GTAGAAGGTCAGGATCAAG-3′ (antisense); hEAG-1 (NM 172362, NM 002238), 5′-CGCATGAACTACCTGAAGACG-3′ (sense) and 5′-TCTGTGGATGGGGCGATGTTC-3 (antisense); mERG-1 (NM_172057), 5′-CCTCGACACCATCATCCGC-3′ (sense) and 5′-GTCCGCACAGATGATTCCC-3′ (antisense); mELK-1 (NM_001031811), 5′-GGTTTCCCCATAGTCTACTG-3′ (sense) and 5′-CAAAATGAGCCAGTCCCAGC-3′ (antisense); mENaCα (NM_011324), 5′-CCTTGACCTAGACCTTGACG-3′ (sense) and 5′- CGAATTGAGGTTGATGTTGAG-3′ (antisense); mENaCβ (NM_000336), 5′-CAATAACACCAACACCCACG-3′ (sense) and 5′- GAGAAGATGTTGGTGGCCTG-3′ (antisense); mENaCγ (NM_011326), 5′-GCACCGACCATTAAGGACC-3′ (sense) and 5′-GCCTTTCCCTTCTCGTTCTC-3′ (antisense); mCFTR (NM_021050), 5′-GAATCCCCAGCTTATCCACG-3′ (sense) and 5′-CTTCACCATCATCTTCCCTAG -3′ (antisense). PCR reactions were done at 94°C for 2 min, 28 to 38 cycles at 94°C for 30 s, annealing temperature of 56°C for 30 s, and 72°C for 1 min using GoTaq DNA Polymerase (Promega, Mannheim, Germany). Expression of mRNA of each gene product was normalized against β-actin expression.

Detection of Eag-1 protein. Isolated crypt cells from distal and proximal colon were lysed, and total protein (50 μg) was resolved by 7% SDS-PAGE, transferred by semi-dry blotting to Hybond-P (Amersham, Freiburg, Germany), and incubated with rabbit anti-Kv10.1 (Eag-1; Alomone Labs, Jerusalem, Israel) and rabbit anti-actin antibodies (Sigma, Taufkirchen, Germany). Proteins were visualized using a goat anti-rabbit IgG conjugated to horseradish peroxidase (Acris Antibodies, Hiddenhausen, Germany) and Enhanced Chemiluminescence Advance Detection kit (Amersham). Signals were detected by Fluor-S MultiImager system (Bio-Rad Laboratories, Hercules, CA) and analyzed with Multi-Analyst software (Bio-Rad Laboratories). Expression of EAG-1 protein was normalized against actin protein expression.

Fluorescence* in situ *hybridization analysis. The bacterial artificial chromosome RP11-75i2, containing parts of the *Eag-1* gene sequence at 1q32.2-3, was obtained from the German Resource Centre for Genome Research (Berlin, Germany). One microgram of purified plasmid DNA was labeled using a modified Bio Nick kit (Invitrogen, Carlsbad, CA). Nick translation was done at 16°C for 90 min. The labeled fluorescence *in situ* hybridization probe was purified by precipitation and redissolved in 50 μL H_2O. Paraffin removal (3 × 5 min in xylene followed by 2 × 2 min ethanol 95% and air-drying) and enzymatic tissue pretreatment (Vysis pretreatment solution, 80°C, 15 min) of tissue sections mounted on glass slides were done in a VP2000 Processor device (Vysis, Downers Grove, IL). A premixed hybridization cocktail containing 0.5 μL centromere 1 probe (CEP 1 SpectrumOrange labeled; Vysis), 1.5 μL Eag-1 probe, 1 μL Cot DNA (Invitrogen), and 7 μL hybridization buffer (Vysis) were added to each slide with denatured target DNA. Probes were allowed to hybridize overnight at 37°C in a humidified chamber. After washing steps, Eag-1 probe was detected using the Dig detection kit (Roche Diagnostics, Indianapolis, IN). Amplification was defined as a signal ratio of Eag-1 probe/centromere 1 of at least two and at least four gene signals.

Materials and statistical analysis. All used compounds were of highest available grade of purity. DMH, MNU, amiloride, 4-aminopyridine, astemizole, carbachol, and 3-isobutyl-1-methylxanthine were from Sigma-Aldrich (Taufkirchen, Germany). DSS was from ICN (Eschwege, Germany). Forskolin and 293B were gifts from Aventis Pharma (Frankfurt, Germany). Student's *t* test (for paired or unpaired samples as appropriate) and ANOVA were used for statistical analysis. $P < 0.05$ was accepted as significant. Survival curves were plotted according to Kaplan-Meier. A log-rank test was applied to examine the relationship between alteration clinicopathologic data or Eag-1 amplification status and overall survival. Patients were censored at the

time of their last clinical control. Cox proportional hazard model with stepwise selection of the covariates was used to determine the variables with greatest influence on the risk of recurrence and progression.

Results

Histopathology. From week 12 on, DMH-treated animals showed a significantly reduced weight increase. MNU-treated mice also showed a reduced body weight and a growth delay compared with untreated mice. Frequently, the animals developed diarrhea upon treatment with carcinogens. Six to 8 weeks after DMH treatment, local mucosal infiltration of leucocytes indicated inflammatory processes in distal colon (Fig. 1A and B). After 10 and 12 weeks, changes of mucosal architecture, such as tortuous crypts and crypt loss, were observed in distal colon (Fig. 1C). No obvious histologic changes were found in the proximal colon. Rectal MNU application four times in 2 weeks induced hyperplastic crypts in distal colon, indicated by an increase of crypt heights and decreased number of globlet cells along the cryptal wall. Moreover, nuclear to cytoplasmic ratio was increased (Fig. 1D). Cellular redistribution and nuclear accumulation of β-catenin was not clearly correlated with carcinogen treatment and was therefore not used as an independent marker for carcinogenesis (data not shown). Mucosal infiltration by inflammatory cells was observed in the proximal colon. After eight treatments (week 6), extension of the lamina submucosae and muscularis submucosae and dysplasia of distal colonic mucosa were observed. Administration of DSS caused severe changes of the tissue architecture, ulceration, and inflammatory cell infiltration, areas of complete epithelial denudation, and submucosal edema in distal and proximal colon. Thus, inflammation and carcinogenesis induced by chemicals are clearly shown by histologic changes.

DMH, MNU, and DSS treatment inhibits Na^+ absorption and Cl^- secretion. In essence, electrogenic ion transport in the colon is due to Na^+ absorption by amiloride-sensitive Na^+ channels (ENaC) and cyclic AMP– or Ca^{2+}-induced Cl^- and K^+ secretion. The amount of electrogenic Na^+ absorption is determined by inhibition with amiloride and calculation of the amiloride-sensitive short circuit current $I_{SC\ Amil}$ (Fig. 2A). DMH treatment reduced $I_{SC\ Amil}$ in distal colon 6 and 8 weeks after the first DMH injection, which recovered at weeks 10 and 12 (Fig. 2A and B). Similar effects on amiloride-sensitive Na^+ absorption were seen in MNU-treated mice. Rectal potential difference measurements *in vivo* after 2 and 6 weeks of MNU treatment showed a reduced rectal potential difference due to attenuated amiloride-sensitive transport (Fig. 2C). Ussing chamber experiments and I_{SC} measurements confirmed reduced Na^+ absorption in distal colon of MNU-treated mice (19.6 ± 4.3 μA/cm^2; $n = 11$), when compared with control mice (57.8 ± 9.6 μA/cm^2; $n = 13$; Fig. 2D). In addition, in the inflamed colon, during treatment with DSS, amiloride-sensitive rectal potential difference was significantly reduced from -7.2 ± 0.58 mV ($n = 7$) to -4.9 ± 0.73 mV ($n = 10$).

Increase in intracellular cyclic AMP (cAMP) by 3-isobutyl-1-methylxanthine (100 μmol/L) and forskolin (2 μmol/L) induced Cl^- secretion ($I_{SC\ cAMP}$) in proximal and distal colon, by activation of the cystic fibrosis transmembrane conductance regulator (CFTR). DMH caused a reduced $I_{SC\ cAMP}$ response in both proximal and distal colon at weeks 6 and 8. In contrast,

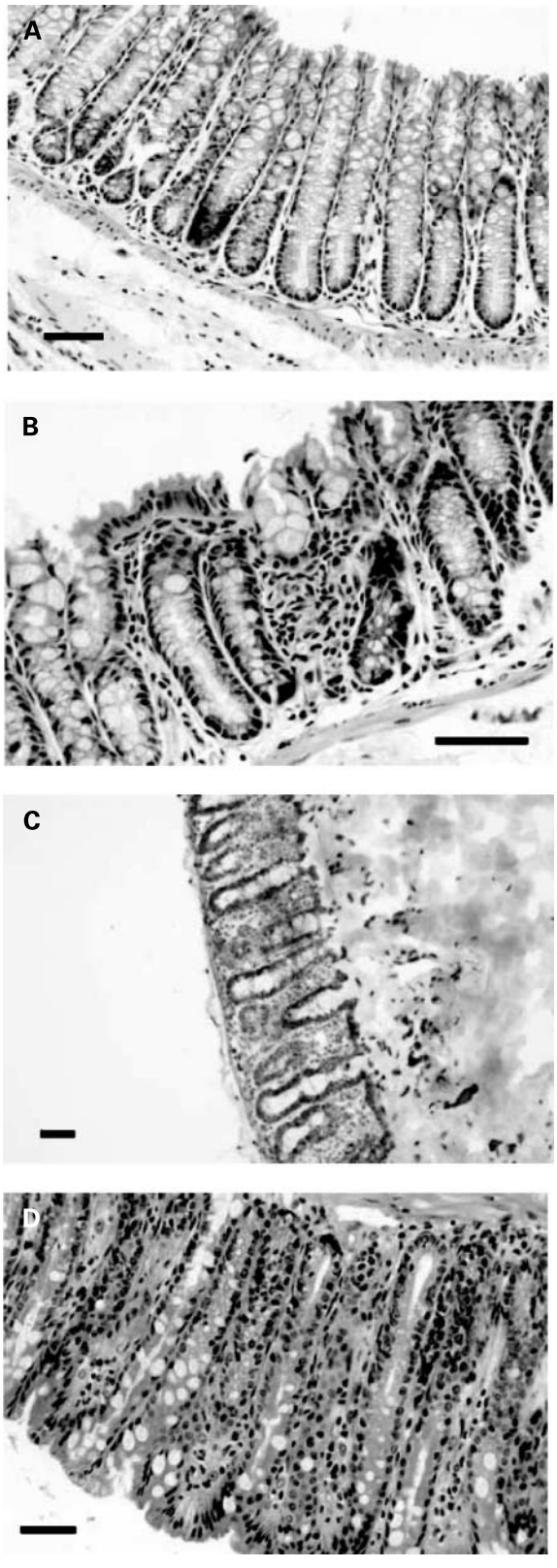

Fig. 1. Effects of DMH, MNU, and DSS treatment on colon architecture. *A,* H&E staining of control distal colon. *B,* infiltration by inflammatory cells of distal colonic mucosa after DMH treatment. *C,* loss of crypts in distal colonic mucosa of DMH-treated mice. *D,* hyperplastic crypts in distal colon after MNU treatment. Bar, 50 μm.

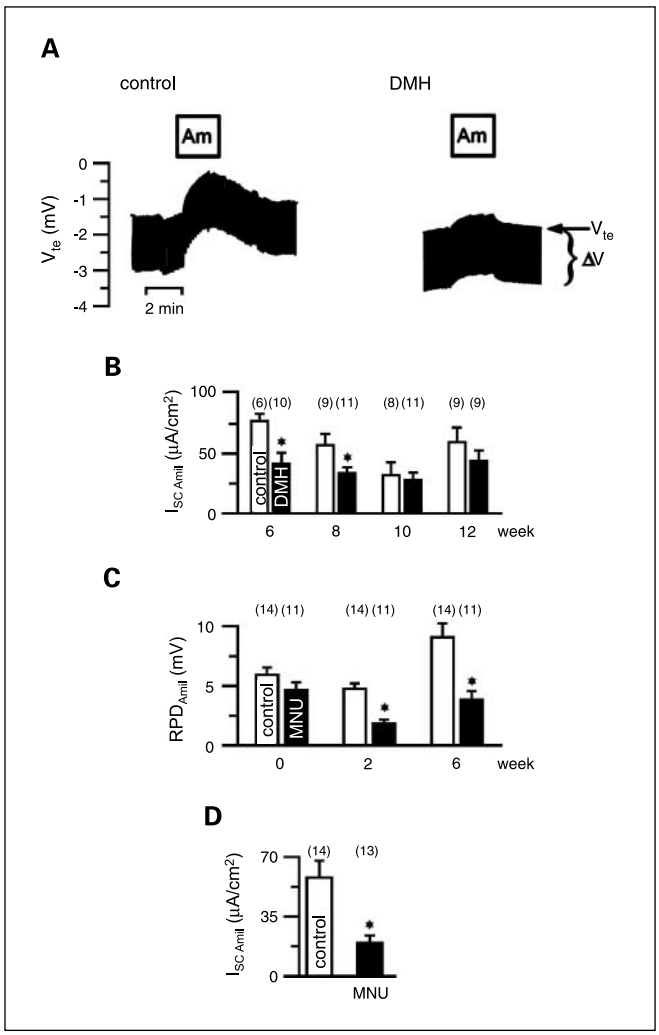

Fig. 2. Change of amiloride-sensitive transport by carcinogens. *A,* Ussing chamber recordings of the transepithelial voltage. Amiloride (*Am*, 20 μmol/L), a specific inhibitor of epithelial Na^+ channels, reduced V_{te} and increased ΔV_{te} due to inhibition of Na^+ absorption. The effect of amiloride on V_{te} was reduced after 6 wks of DMH treatment. *B,* amiloride (20 μmol/L) – sensitive I_{SC} ($I_{SC\ Amil}$) was reduced in Ussing chamber experiments 6 and 8 wks after initial DMH injection. *C,* rectal potential difference (*RPD*) measurements showed reduced effects of amiloride (RPD_{Amil}) 2 and 6 wks after rectal application of MNU. *D,* Ussing chamber experiments confirmed reduced $I_{SC\ Amil}$ in distal colon 6 wks after rectal application of MNU. *, significant differences compared with control (Student's *t* test). Number of mice in brackets.

later-stage (week 12) $I_{SC\ cAMP}$ was significantly elevated in proximal colon (Fig. 3A and B). It is well known that basolateral cAMP- dependent activation of the cotransporter NKCC1 and 293B-sensitive KCNQ1 K^+ channels ($I_{SC\ 293B}$) facilitate CFTR-dependent Cl^- secretion. Accordingly, DMH treatment inhibited $I_{SC\ 293B}$ in cAMP-stimulated proximal colon at week 6 and increased $I_{SC\ 293B}$ at week 12 (Fig. 3C). Similar to DMH in the early phase, MNU and DSS also reduced cAMP-dependent Cl^- secretion in rectal potential difference measurements (Fig. 3D). This was further confirmed in Ussing chamber recordings. Here, cAMP-activated transport was significantly attenuated by 62.3 ± 5.3 μA/cm² (n = 14) in MNU-treated animals and by 174.3 ± 18.2 μA/cm² (n = 7) in DSS-treated mice. In contrast, Ca^{2+}-activated Cl^- secretion, stimulated by carbachol (100 μmol/L) and blockage by niflumic acid (100 μmol/L), remained unchanged (data not shown). Hence, electrogenic Na^+ absorption via ENaC and cAMP-dependent Cl^- secretion by CFTR are changed during inflammation and carcinogenesis, whereas Ca^{2+}-activated Cl^- secretion remains unaffected. Because both ENaC and CFTR are the major determinants for net fluid transport in the colon, these changes are likely to affect digestive functions of the colon.

Carcinogens induce voltage-gated K^+ channels. A major goal of the present study was to identify potential oncogenic ion channels during inflammation and carcinogenesis of the colonic epithelium. It is well established that proliferation of cancer cells and metastasis require the activity of plasma membrane K^+ channels (1, 2). We investigated the function of Kv channels in the premalignant colon using the nonselective Kv channel inhibitor 4-aminopyridine (100 μmol/L) and the inhibitor of the Eag channel family, astemizole (5 μmol/L). Application of both 4-aminopyridine and astemizole had only minor effects on I_{SC} in control animals but inhibited I_{SC}

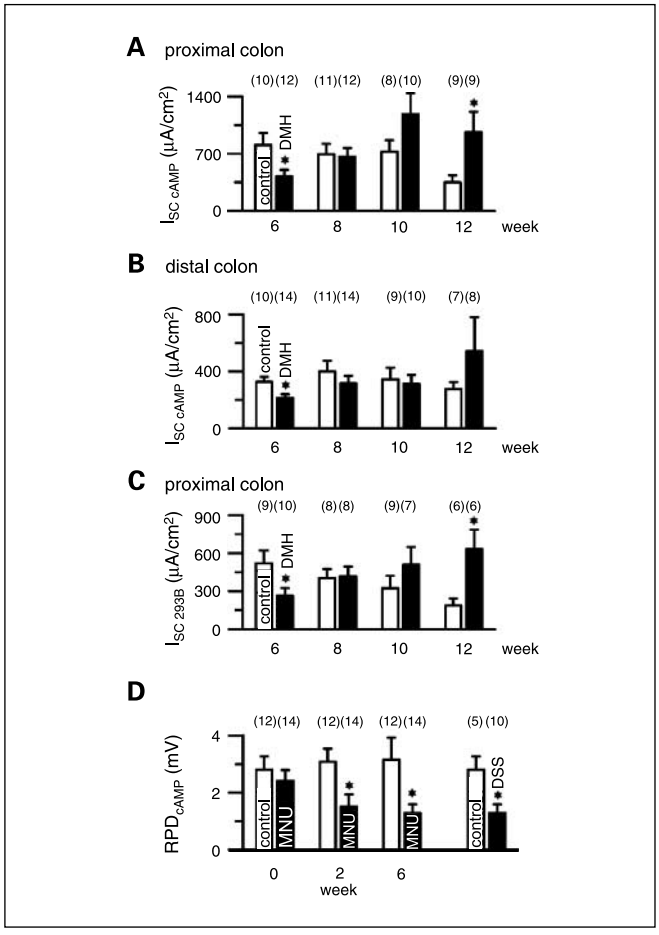

Fig. 3. Treatment with DMH, MNU, and DSS reduced CFTR-dependent Cl^- secretion. *A,* 3-isobutyl-1-methylxanthine and forskolin increased intracellular cAMP and activated CFTR-dependent Cl^- secretion. In proximal colon, cAMP-induced I_{SC} ($I_{SC\ cAMP}$) was reduced 6 wks after DMH injection but was elevated after 12 wks. *B,* summary of the effects of DMH on $I_{SC\ cAMP}$ in distal colon. *C,* the 293B-sensitive I_{SC} ($I_{SC\ 293B}$) was reduced 6 wks after DMH injection and was elevated after 12 wks. *D,* increase in rectal potential difference by 3-isobutyl-1-methylxanthine and forskolin (RPD_{cAMP}) was reduced in MNU- and DSS-treated mice, respectively. *, significant differences compared to control (Student's *t* test). Number of mice in brackets.

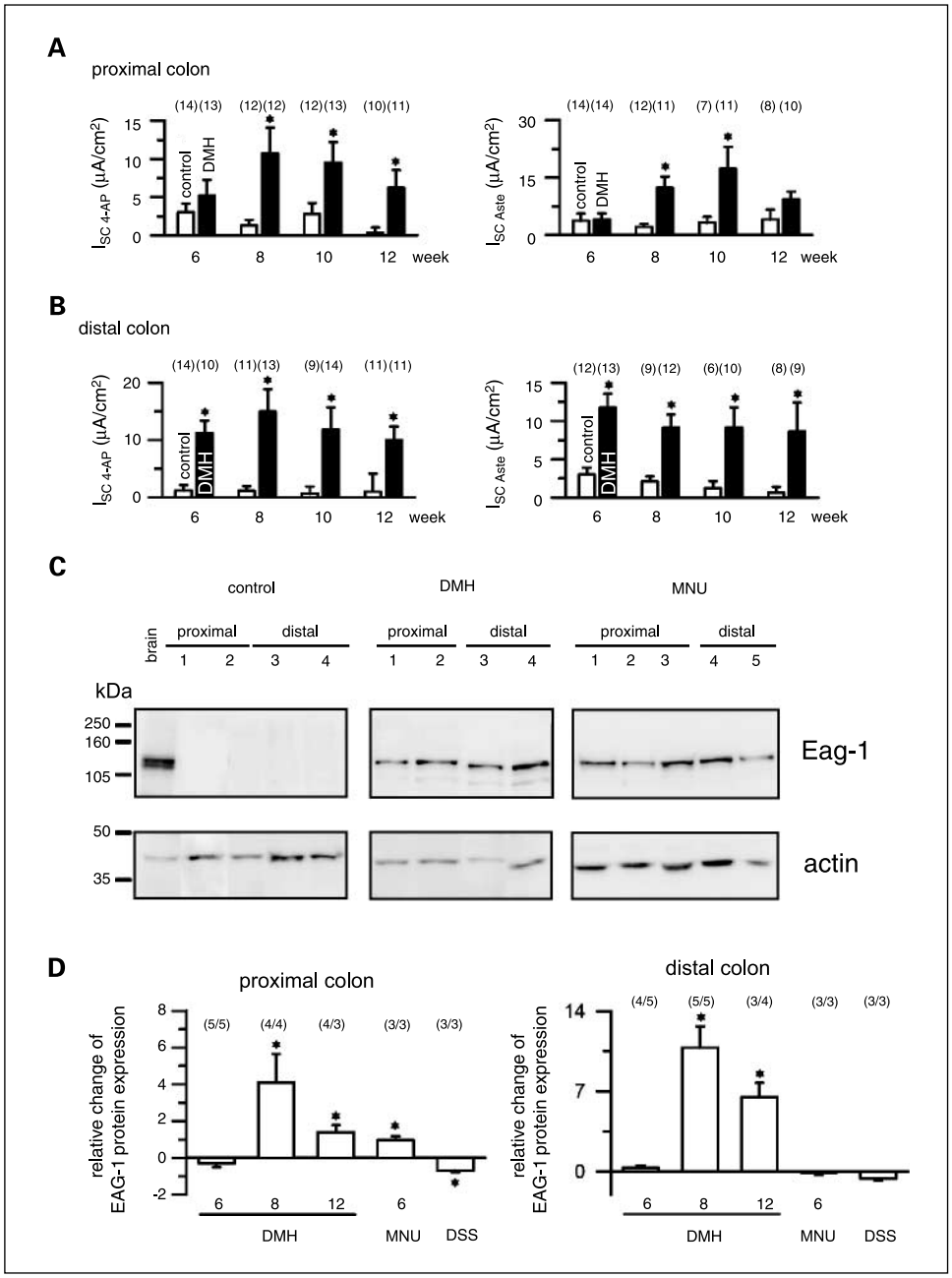

Fig. 4. Treatment with carcinogens enhanced expression of voltage-gated K^+ channels. In proximal (*A*) and distal (*B*) colon, application of 4-aminopyridine and astemizole indicated enhanced activity of voltage-gated K^+ channels after treatment with carcinogens. *C,* Western blot analysis of Eag-1 (111 kDa) and β-actin (42 kDa) expression in brain (positive control) and crypt cells of proximal and distal colon of control and DMH- and MNU-treated mice. *D,* summary of the changes in Eag-1 expression (normalized against β-actin) in crypt cells of DMH-, MNU-, and DSS-treated mice. *, significant differences compared with control (Student's *t* test). Number of mice in brackets.

significantly in proximal and distal colon of DMH-treated mice (Fig. 4A and B). These results suggest that DMH treatment induced activation of Kv and Eag-related K^+ channels in both distal and proximal colon. Similar results were obtained in distal colon of MNU-treated mice, where I_{SC} was significantly reduced by 4.3 ± 0.54 μA/cm² (n = 14). The inflamed (DSS) colon did not exhibit Kv channel activity in Ussing chamber recordings and showed only small rectal potential difference changes upon application of 4-aminopyridine (data not shown). In summary, Kv channels and cell cycle–regulated Eag channels were clearly detected in the premalignant colon but were absent in the inflamed colon.

Expression of ion channel mRNA in crypt cells of DMH-, MNU-, and DSS-treated mice. Because we detected changes in electrolyte transport and enhanced Kv channel activity in the premalignant colon, we investigated molecular expression of the underlying ion channels. Total RNA was prepared from freshly isolated crypt cells of proximal and distal colon of DMH-, MNU-, and DSS-treated (each n = 6) animals and control mice. Changes in ion channel expression relative to the control group were calculated. We found a small but significant increase in the mRNA expression for α, β, and γ subunits of ENaC in DMH-treated animals. No changes in expression of CFTR could be detected (Table 1). Thus, changes in Na^+ absorption and Cl^- secretion due to the DMH treatment are not explained by changes in transcript expression of the respective ion channels but are due to other secondary changes (cf. Discussion). Enhanced 4-aminopyridine–sensitive K^+ currents detected in carcinogen-treated animals may also be caused by enhanced expression of Kv channels. In fact, mRNAs

Table 1. Changes in ion channel mRNA expression in crypt cells of proximal and distal colon of DMH-, MNU-, and DSS-treated mice

Gene	DMH wk 6	DMH wk 8	DMH wk 10	DMH wk 12	MNU wk 6	DSS
Proximal colon						
ENaC α	NC (5/6)	NC (4/6)	NC (6/6)	−0.57 ± 0.06 (4/5)*	NC (6/6)	NC (4/6)
ENaC β	−0.45 ± 0.08 (5/5)*	NC (6/6)	NC (6/5)	2.65 ± 0.97 (5/6)*	NC (5/6)	NC (4/6)
ENaC γ	NC (6/5)	NC (6/4)	NC (6/5)	9.75 ± 4.27 (5/5)*	NC (6/6)	2.21 ± 0.62 (4/6)*
CFTR	NC (5/6)	−0.77 ± 0.07 (4/5)*	NC (6/5)	NC (6/6)	NC (6/6)	NC (4/6)
Kv1.3	NC (5/6)	13.59 ± 4.27 (4/6)*	NC (6/6)	NC (5/6)	NC (6/6)	NC (4/6)
Kv1.5	NC (6/6)	NC (6/6)	NC (6/6)	NC (5/5)	3.13 ± 0.85 (5/6)*	NC (4/6)
Kv3.1	NC (3/3)	6.19 ± 1.64 (3/3)*	1.36 ± 0.43 (6/6)*	4.03 ± 1.31 (4/5)*	1.41 ± 0.60 (6/6)*	NC (4/6)
EAG-1	NC (5/6)	NC (5/4)	2.04 ± 0.59 (4/4)*	8.15 ± 2.06 (4/5)*	NC (6/6)	NC (4/6)
ERG-1	1.96 ± 0.80 (6/6)*	6.44 ± 2.17 (3/3)*	8.64 ± 1.47 (3/3)*	30.38 ± 2.81 (3/3)*	NC (6/6)	NC (4/6)
ELK-1	NC (6/6)	1.09 ± 0.37 (5/5)*	2.83 ± 1.42 (5/3)*	2.25 ± 0.76 (4/5)*	−0.73 ± 0.14 (5/6)*	NC (3/6)
Distal colon						
ENaC α	NC (6/6)	NC (5/5)	NC (6/6)	−0.54 ± 0.08 (5/4)*	NC (6/6)	−0.79 ± 0.08 (4/5)*
ENaC β	−0.55 ± 0.09 (5/6)*	NC (5/5)	NC (6/6)	2.54 ± 0.56 (5/6)*	NC (6/5)	NC (4/6)
ENaC γ	NC (6/5)	NC (5/5)	NC (6/6)	5.60 ± 2.22 (5/5)*	NC (6/5)	1.14 ± 0.47 (4/4)*
CFTR	NC (5/6)	0.61 ± 0.11 (5/6)*	NC (6/6)	NC (6/6)	NC (6/6)	NC (4/6)
Kv1.3	NC (6/6)	NC (6/6)	NC (6/6)	NC (5/6)	15.32 ± 7.48 (5/4)*	4.13 ± 1.57 (4/5)*
Kv1.5	7.52 ± 1.86 (6/6)*	NC (6/6)	NC (6/6)	NC (5/5)	NC (6/6)	NC (4/6)
Kv3.1	NC (3/3)	1.80 ± 0.65 (3/3)*	0.93 ± 0.29 (3/3)*	1.06 ± 0.17 (3/3)*	NC (6/5)	NC (4/6)
EAG-1	NC (6/6)	NC (5/5)	NC (6/5)	2.65 ± 0.83 (4/4)*	NC (6/6)	NC (3/6)
ERG-1	4.44 ± 0.37 (3/3)*	NC (5/5)	1.41 ± 0.22 (3/3)*	2.78 ± 2.12 (3/2)*	2.78 ± 1.14 (6/6)*	NC (4/6)
ELK-1	NC (6/6)	NC (6/6)	NC (6/6)	NC (6/6)	NC (5/5)	NC (4/6)

NOTE: Expression of mRNA was normalized against β-actin expression, and changes relative to the control group were calculated. Number of mice is given in parentheses.
Abbreviation: NC, no change.
*Significant difference to control (Student's *t* test).

encoding the channels Kv3.1, Kv1.3, and Kv1.5 were clearly up-regulated in both distal and proximal colonic crypt cells of DMH- and MNU-treated animals. Moreover, corresponding to the enhanced astemizole-sensitive currents (Fig. 4A and B), we detected enhanced mRNA expression of ether a go-go subtypes Eag-1, Erg-1, and Elk-1 in the premalignant proximal and distal colon of DMH- and MNU-treated mice but not in the inflamed (DSS) colon (Table 1).

DMH and MNU treatment increased expression of Eag-1 protein. Cell cycle–dependent regulation of Eag-1 is well established; thus far, expression of the channel was only found in cancer cells but not in normal epithelial tissues (7). Because

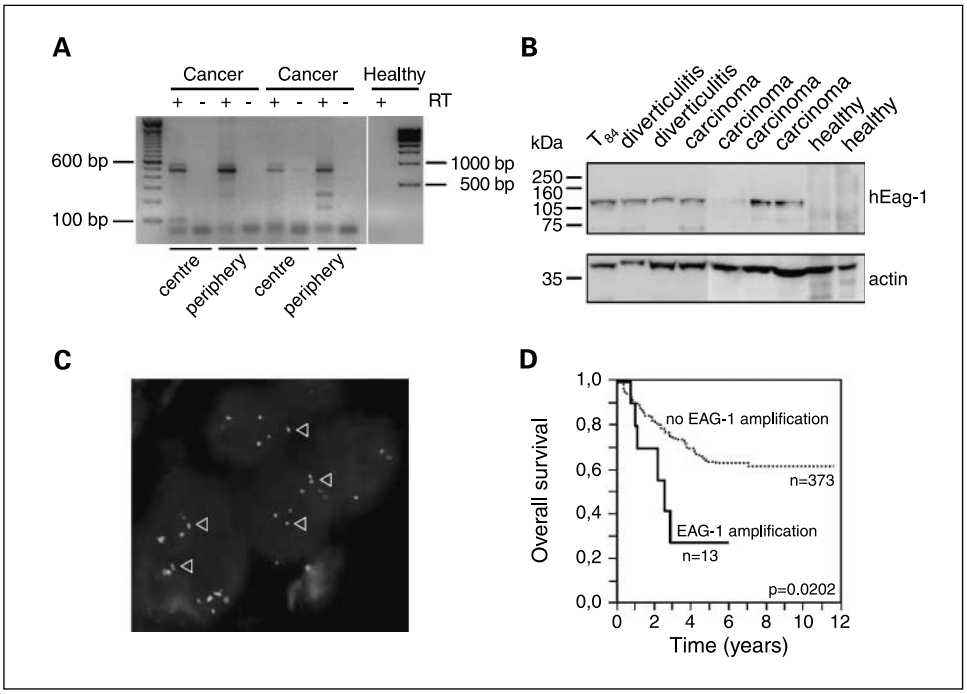

Fig. 5. Eag-1 is expressed in colonic crypt cells of patients with cancer and diverticulitis. *A,* reverse transcription-PCR showed mRNA expression of the two variants of Eag-1 (variant 1, 560 bp; variant 2, 479 bp) in the center and peripheral tissue of the cancer in two patients. In a colon biopsy of a healthy volunteer, no Eag-1 transcripts were detected. *B,* total protein was isolated from T84 colonic cancer cells and from crypt cells derived from patients with different diagnosis. Colonic biopsies of healthy patients served as controls. *C,* fluorescence *in situ* hybridization of a colorectal adenocarcinoma with Eag-1 amplification. Tumor cell nuclei contain numerous green Eag-1 signals but only few reference signals in red (centromere 1; ×1,000). Nuclei counterstained with DAPI (*blue*). *D,* effect of *Eag-1* gene amplification on overall survival in surgically resected colorectal adenocarcinoma.

DMH treatment induced an astemizole-sensitive I_{SC} and increased Eag-1 mRNA expression in proximal and distal colon, we also examined protein expression in isolated crypt cells. In the control group, Western blot analysis showed no uniform Eag-1 expression in crypt cells (Fig. 4C). In contrast, in crypt cells of DMH-treated mice, Eag-1 protein was well detected in proximal and distal colon (Fig. 4C). The carcinogen MNU enhanced Eag-1 expression in the proximal colon, whereas no changes were observed in the inflamed colon (DSS), as indicated by densitometric analysis relative to actin staining (Fig. 4D).

Eag-1 protein expression in human carcinomas and diverticulitis. Eag-1 expression was analyzed by reverse transcription-PCR in biopsies of two colorectal carcinomas, and the Eag-1 transcript variants 1 and 2 were found in the center of the carcinoma and in the macroscopically unaffected periphery. However, no expression of Eag-1 mRNA was found in the colon of a healthy volunteer (Fig. 5A). Expression of Eag-1 protein was analyzed in isolated crypt cells from patients diagnosed with sigma diverticulitis, ulcerative colitis, colorectal adenocarcinoma, cecum carcinoma, and colonic neoplasm (Fig. 5C). Samples were also obtained from patients with unrelated diseases, such as cystic fibrosis. No expression of Eag-1 was detected in these samples. The variability of the tissue sample quality was assessed by simultaneous detection of β-actin expression. In summary, expression of Eag-1 was detected in most carcinomas and in some patients diagnosed with diverticulitis, whereas the healthy colon does not seem to express cell cycle–regulated K^+ channels (Fig. 5B).

The* Eag-1 *gene is amplified in tumor specimens and is associated with adverse outcome. Pathologic tumor-node-metastasis stage, histologic grade, and International Union Against Cancer stage were strongly associated with overall survival ($P < 0.0001$ each; data not shown). Fluorescence *in situ* hybridization analysis showed amplification of the *EAG-1* gene in 13 (3.4%) of the 386 tumor specimens (Table 2). A representative case with EAG-1 amplification is shown in Fig. 5C. Univariate survival analysis revealed that EAG-1 amplification was significantly associated with adverse outcome ($P = 0.0202$; Fig. 5D). If entered in a multivariate model (Cox proportional hazard), amplification of EAG-1 emerged as an independent prognostic marker ($P = 0.0126$; relative risk, 3.55) together with International Union Against Cancer stage ($P < 0.0001$; relative risk, 15.56) and histologic grade ($P = 0.0167$; relative risk, 1.77; $n = 386$). Thus, expression of Eag-1 is associated with reduced overall survival in patients with colonic carcinoma.

Discussion

Effects of proinflammatory and carcinogenic chemicals. For the present study, we used the mouse C57BL/6N strain, which shows a high incidence of colorectal tumors after DMH treatment (16, 17). Histologic changes were identified early after DMH injection; however, definite cancers develop typically only after 24 weeks of treatment (17). Intrarectal infusion of MNU yielded a high incidence (up to 100%) of colon cancer in previous studies with shrews (18). We detected initial inflammatory responses in both DMH- and MNU-treated animals, similar to the inflamed (DSS) colon. However, at later stages, carcinogens caused significant changes in mucosal architecture and expression of Kv3.1, Kv1.3, and Kv1.5 and, particularly, Eag channels. This was not observed in the DSS model. Thus, expression of oncogenic Eag channels seem to be a consequence of the carcinogen treatment and not simply a result from inflammation. This channel was also found in human colonic cancers but not in normal tissues. It suggests that Eag has an oncogenic potential in the colonic epithelium. Interestingly, Eag was also detected in diverticulitis, which has the potential to change into colonic cancer. We hypothesize that expression of Eag in preneoplastic tissues supports malignancy and may drive the development towards colonic cancer.

Electrolyte transport changes during carcinogenesis and colitis. Several reports show altered electrolyte transport in early stages of tumor development. Using the present models, we confirm reduction of amiloride-sensitive Na^+ absorption by treatment with DMH, MNU, and DSS. Inhibition of amiloride-sensitive Na^+ absorption was not explained by changes in the expression profile of the three Na^+ channel subunits. A likely reason for reduced Na^+ absorption is an attenuation of the Na^+/K^+-ATPase in the distal colon (19). cAMP-induced Cl^- secretion was reduced initially but was up-regulated at later stages of DMH treatment. Stool irregularities, with changes from constipation to diarrhea, are often observed in patients with intestinal tumors or inflammatory bowel disease, and the present findings may, therefore, supply an explanation for these symptoms.

Expression of Kv channels during inflammation and carcinogenesis. Kv channels promote cell proliferation and support tumor development (2, 3). In multiplex reverse transcription-PCR, we found enhanced expression of the channels Kv1.3,

Table 2. Clinicopathologic characteristics of colorectal adenocarcinomas ($n = 386$)

Sex	
M	200 (48.1%)
F	186 (51.8%)
Age (range), y	71.6 ± 1.1 (36-96)
Localization	
Right colon	164 (43.4%)
Left colon	214 (56.6%)
pT	
pT_1	7 (1.8%)
pT_2	64 (16.6%)
pT_3	247 (64.0%)
pT_4	68 (17.6 %)
pN	
pN_0	195 (50.5%)
pN_1	107 (28.2%)
PN_2	84 (27.7%)
pM	
pM_0	309 (80.1%)
PM_1	77 (19.9%)
Stage	
I	53 (13.7%)
II	129 (33.4%)
III	127 (32.9%)
IV	77 (20.0%)
Grading	
G1	2 (0.5%)
G2	290 (75.1%)
G3	94 (24.4%)
Follow-up (mo)	
Mean (range)	37.7 ± 3.4 (0-140)
Median	31.0

Kv1.5, and Kv3.1 (Table 1). Kv1.3 (gene locus *KCNA3*) is essential for lymphocyte proliferation and supports development of cancer in prostate, colon, and breast. Kv1.5 (gene locus *KCNA5*) supports proliferation of gastric cancer (1, 20). Moreover, expression of Kv1.5 correlates with the grade of malignancy of gliomas (21). The apparent dissociation constants (K_d) of 4-aminopyridine for Kv1.3, Kv1.5, and Kv3.1 channels are 195, 270, and 29 μmol/L, respectively, which are in the range of the 4-aminopyridine concentration (100 μmol/L) used in the present study (22). We suggest that Kv3.1 (gene locus *KCNC1*) is mainly responsible for the 4-aminopyridine–dependent inhibition of ion transport in the malignant colon. Thus, this is the first study that supplies evidence that Kv3.1 channels are involved in development of cancer. Expression of Kv3.1 is normally restricted to the central nervous system and to a subpopulation of T lymphocytes (2). Kv3.4, another member of this subfamily of Kv channels, controls proliferation of oral and esophageal squamous carcinoma cells (23).

An oncogenic role of EAG channels in the colon. According to previous reports, expression of Eag-1 and Erg-1 channels is strictly limited to excitable tissues. In contrast, in malign epithelial tumors, the cell cycle–controlled Eag channel determines malignancy and metastasis of breast cancer (2, 4, 7, 24). Crypt cells of carcinogen-treated mice showed expression of Eag-1, Erg-1, and Elk-1 in the present study. When normalized to the actin signal, expression of Eag-1 was somewhat larger in the distal colon when compared with the proximal colon of DMH-treated animals. However, the difference was not statistically different. Moreover, expression of Eag-1 was found in human colorectal adenocarcinomas. Fluorescence *in situ* hybridization analysis showed amplification of the *EAG-1* gene in 13 (3.4%) of the 386 tumor specimens. EAG-1 amplification was significantly associated with adverse outcome. The low prevalence of EAG-1 amplification does not question its importance because mechanisms other than amplification may account for activation and overexpression in a larger fraction of tumors. For example, another potassium channel, KCNK9 at 8q24.3, was previously found to be amplified in ~10%, but overexpressed in 44%, of breast cancers (25).

Taken together, carcinogenesis in the colon and colitis change expression of ion channels important for salt transport, which is likely to cause stool irregularities. Expression of the cell cycle–regulated K^+ channel Eag-1 is closely correlated with malignancy in the human and rodent colon, and *Eag-1* gene amplification is associated with reduced surviving rate. These data suggested that Eag-1 expression is important for tumor development in the human colon. Because Eag-1 is already expressed at a premalignant stage, Eag-1 transcripts detected in rectal biopsies or stool samples may serve as early diagnostic and prognostic markers, as shown recently for cervical cancer (6). The present data may also be useful in developing new therapeutic strategies for the treatment of colonic cancer.

Acknowledgments

We thank Drs. F. Obermeier and Frauke Bataille (Department of Medicine I and Pathology, University of Regensburg, Germany) for supplying DSS mice and for help with histology, Ernestine Tartler and Agnes Paech for their excellent technical assistance, Dr. Michel Bloch and Hedvika Novotny (Institute for Pathology, University Basel) for their expert help with fluorescence *in situ* hybridization analysis, and Dr. Marcus Mall (Kinderklinik der Universität Heidelberg, Germany) for providing tissue samples.

References

1. Kunzelmann K. Ion channels and cancer. J Membr Biol 2005;205:159–73.
2. Pardo LA. Voltage-gated potassium channels in cell proliferation. Physiology (Bethesda) 2004;19:285–92.
3. Pardo LA, Contreras-Jurado C, Zientkowska M, et al. Role of voltage-gated potassium channels in cancer. J Membr Biol 2006;205:115–24.
4. Camacho J. Ether a go-go potassium channels and cancer. Cancer Lett 2006;233:1–9.
5. Wonderlin WF, Strobl JS. Potassium channels, proliferation and G_1 progression. J Membr Biol 1996;154:91–107.
6. Farias LM, Ocana DB, Diaz L, et al. Ether a go-go potassium channels as human cervical cancer markers. Cancer Res 2004;64:6996–7001.
7. Pardo LA, del Camino D, Sanchez A, et al. Oncogenic potential of EAG K^+ channels. EMBO J 1999;18:5540–7.
8. Schreiber R. Ca^{2+} signaling, intracellular pH and cell volume in cell proliferation. J Membr Biol 2005;205:129–37.
9. Fiala ES. Investigations into the metabolism and mode of action of the colon carcinogens 1,2-dimethylhydrazine and azoxymethane. Cancer 1977;40:2436–45.
10. Frei JV, Swenson DH, Warren W, et al. Alkylation of deoxyribonucleic acid *in vivo* in various organs of C57BL mice by the carcinogens *N*-methyl-*N*-nitrosourea, *N*-ethyl-*N*-nitrosourea and ethyl methanesulphonate in relation to induction of thymic lymphoma. Some applications of high-pressure liquid chromatography. Biochem J 1978;174:1031–44.
11. Narisawa T, Wong CQ, Maronpot RR, et al. Large bowel carcinogenesis in mice and rats by several intrarectal doses of methylnitrosourea and negative effect of nitrite plus methylurea. Cancer Res 1976;36:505–10.
12. Davies RJ, Weidema WF, Sandle GI, et al. Sodium transport in a mouse model of colonic carcinogenesis. Cancer Res 1987;47:4646–50.
13. Bleich M, Ecke D, Schwartz B, et al. Effects of the carcinogen dimethylhydrazine (DMH) on the function of rat colonic crypts. Pflügers Arch 1997;433:254–9.
14. Kononen J, Bubendorf L, Kallioniemi A, et al. Tissue microarrays for high-throughput molecular profiling of tumor specimens. Nat Med 1998;4:844–7.
15. Sobin L, Wittekind C. UICC TNM classification of malignant tumors. Vol. 75. New York: Wiley; 2002.
16. Diwan BA, Blackman KE. Differential susceptibility of 3 sublines of C57BL/6 mice to the induction of colorectal tumors by 1,2-dimethylhydrazine. Cancer Lett 1980;9:111–5.
17. Greene FL, Lamb LS, Barwick M. Colorectal cancer in animal models: a review. J Surg Res 1987;43:476–87.
18. Yang J, Shikata N, Mizuoka H, et al. Colon carcinogenesis in shrews by intrarectal infusion of *N*-methyl-*N*-nitrosourea. Cancer Lett 1996;110:105–12.
19. Davies RJ, Sandle GI, Thompson SM. Inhibition of the Na^+,K^+-ATPase pump during induction of experimental colon cancer. Cancer Biochem Biophys 1991;12:81–94.
20. Abdul M, Hoosein N. Voltage-gated potassium ion channels in colon cancer. Oncol Rep 2002;9:961–4.
21. Preussat K, Beetz C, Schrey M, et al. Expression of voltage-gated potassium channels Kv1.3 and Kv1.5 in human gliomas. Neurosci Lett 2003;346:33–6.
22. Grissmer S, Nguyen AN, Aiyar J, et al. Pharmacological characterization of five cloned voltage-gated K^+ channels, types Kv1.1, 1.2, 1.3, 1.5, and 3.1, stably expressed in mammalian cell lines. Mol Pharmacol 1994;45:1227–34.
23. Chang KW, Yuan TC, Fang KP, et al. The increase of voltage-gated potassium channel Kv3.4 mRNA expression in oral squamous cell carcinoma. J Oral Pathol Med 2003;32:606–11.
24. Stuhmer W, Alves F, Hartung F, et al. Potassium channels as tumour markers. FEBS Lett 2006;580:2850–2.
25. Mu D, Chen L, Zhang X, et al. Genomic amplification and oncogenic properties of the KCNK9 potassium channel gene. Cancer Lett 2003;3:297–302.